

Constraints on the topology of the Universe derived from the 7-year *WMAP* data

P. Bielewicz¹ *, A. J. Banday¹

¹ *Centre d'Etude Spatiale des Rayonnements, 9, av du Colonel Roche, BP 44346, 31028, Toulouse, France*

10 November 2018

ABSTRACT

We impose constraints on the topology of the Universe determined from a search for matched circles in the temperature anisotropy patterns of the 7-year *WMAP* data. We pay special attention to the sensitivity of the method to residual foreground contamination of the sky maps, and show that for a full sky estimate of the CMB signal (the ILC map) such residuals introduce a non-negligible effect on the statistics of matched circles. In order to reduce this effect, we perform the analysis on maps for which the most contaminated regions have been removed. A search for pairs of matched back-to-back circles in the higher resolution *WMAP* W-band map allows tighter constraints to be imposed on topology. Our results rule out universes with topologies that predict pairs of such circles with radii larger than $\alpha_{\min} \approx 10^\circ$. This places a lower bound on the size of the fundamental domain for a flat universe of about 27.9 Gpc. This bound is close to the upper limit on the size of Universe possible to detect by the method of matched circles, i.e. the diameter of the observable Universe is 28.3 Gpc.

Key words: cosmic background radiation — cosmology: observations

1 INTRODUCTION

According to General Relativity, the pseudo-Riemannian manifold with signature (3,1) is a mathematical model of spacetime. The local properties of spacetime geometry are described by the Einstein gravitational field equations. However, they do not specify the global spatial geometry of the universe, i.e. its topology. This can only be constrained by observations.

The concordance cosmological model assumes that the universe possesses a simply-connected topology, yet recently detected anomalies on large angular scales in the cosmic microwave background (CMB) anisotropy suggest that it may be multiply-connected. Evidence of such anomalies comes from the suppression of the quadrupole moment, alignment of the quadrupole and octopole and asymmetry in the temperature anisotropy observed in two hemispheres on the sky (de Oliveira-Costa et al. 2004; Copi et al. 2004; Eriksen et al. 2004; Hansen et al. 2004; Schwarz et al. 2004).

The present constraints on topology were placed by studying two signatures of multi-connectedness in the CMB maps: the large scale damping of the power in the direction of a small dimension of the domain, which causes a breakdown of statistical isotropy (de Oliveira-Costa et al. 2004;

Kunz et al. 2006, 2008), and the distribution of matched patterns (Cornish et al. 2004; Aurich, Lustig, & Steiner 2005, 2006; Then 2006; Key et al. 2007).

In this work, we constrain the topology of the Universe using the method of matched circles proposed by Cornish, Spergel, & Starkman (1998) and apply it to the 7-year *WMAP* data (Jarosik et al. 2010). In contrast to the majority of previous studies, we will pay special attention to the impact of Galactic foreground residuals on the constraints. Some consideration of this problem was made by Then (2006) in their analysis of the first year *WMAP* data release. We will use also Monte Carlo (MC) simulations for the estimation of the false detection level of the statistic. The method is applied to higher resolution maps than previously, which implies a lower level of false detection and therefore tighter constraints on the size of the Universe. As a result of computational limitations, we will restrict the analysis to a search for back-to-back circle pairs¹.

In the following two sections we describe data used in analysis and simulations of the CMB maps for a flat universe with the topology of a 3-torus which were used to test the reliability of our implementation. The statistic adopted in our studies is presented in Section 4. The results and conclusions are described in the last two sections.

* E-mail: Pawel.Bielewicz@cesr.fr

¹ pairs of circles centred around antipodal points

2 DATA

The search for matched circles was performed on the 7-year *WMAP* data (Jarosik et al. 2010). The *WMAP* satellite observes the sky in five frequency bands denoted K , Ka , Q , V and W , centred on the frequencies of 22.8, 33.0, 40.7, 60.8, 93.5 GHz with angular resolutions of 52.8', 39.6', 30.6', 21' and 13.2', respectively. The maps² are pixelized in the HEALPIX³ scheme (Górski et al. 2005) with a resolution parameter $N_{\text{side}} = 512$, corresponding to 3 145 728 pixels with a pixel size of ~ 7 arcmin.

In particular we used the Internal Linear Combination (ILC) map and the W-band map corrected for Galactic emission outside of the applied mask using a template fitting scheme (Gold et al. 2010) and smoothed with a gaussian beam profile of full width at half-maximum (FWHM) = 20' to decrease noise level. The former has been used for a number of full sky analyses, and versions available with earlier data releases have already been exploited in the search for matched circles. The latter is the highest angular resolution data measured by the *WMAP* satellite. Since the false detection level for such a map is lower, it provides the opportunity to estimate tighter constraints on topology. We elected not to use data preprocessed as in Cornish et al. (2004), i.e. a noise-weighted combination of the Q, V and W-band maps smoothed to Q-band map resolution outside of the Kp2 Galactic cut, and the ILC map within this region. Such a map has complex properties since it consists of two regions with different angular resolutions; moreover, as we will see the ILC map remains too contaminated by Galactic foreground residuals inside the Kp2 cut to be used for cosmological analysis.

3 SIMULATIONS OF THE CMB ANISOTROPY MAPS IN THE MULTI-CONNECTED UNIVERSE

To test the reliability of codes used to search for the signature of a multi-connected topology in the Universe, we performed simulations of CMB skies for a flat universe with the topology of a 3-torus (Riazuelo et al. 2004a). The simulations can be made in two ways: one can compute the covariance matrix⁴ of the spherical harmonic coefficients $a_{\ell m}$, $\mathbf{M}_{\ell m, (\ell m)'} \equiv \langle a_{\ell m} a_{\ell' m'}^* \rangle$, (Riazuelo et al. 2004b; Phillips & Kogut 2006) and then generate correlated $a_{\ell m}$ coefficients using the Choleski decomposition of the covariance matrix $\mathbf{M} = \mathbf{L}\mathbf{L}^\dagger$ and uncorrelated unit variance Gaussian variable \mathbf{x} , $\mathbf{a} = \mathbf{L}\mathbf{x}$, or one can directly compute the $a_{\ell m}$ coefficients using equation

$$a_{\ell m}^T = -\frac{(2\pi)^3}{V} i^\ell \sum_k \Delta_\ell^T(k, \Delta\tau) \frac{\sqrt{P(k)}}{k^2} \sum_{|\mathbf{k}|=k} Y_{\ell m}^*(\Omega_{\mathbf{k}}) \hat{e}_{\mathbf{k}} \quad (1)$$

where $\Delta\tau = \tau_0 - \tau_r$ is difference between the present conformal time τ_0 and the time of recombination τ_r , $P(k)$ is the density perturbation power spectrum, $\Delta_\ell^T(k, \Delta\tau)$ is the response function for temperature, $\hat{e}_{\mathbf{k}}$ is a Gaussian random

variable which satisfies $\langle \hat{e}_{\mathbf{k}} \hat{e}_{\mathbf{k}'}^* \rangle = \frac{V}{(2\pi)^3} \delta_{\mathbf{k}\mathbf{k}'}$ and V is the volume of the fundamental domain. The sum over wavevectors \mathbf{k} was split into two sums $\sum_{\mathbf{k}} = \sum_k \sum_{|\mathbf{k}|=k}$ – the sum over all possible magnitudes of the \mathbf{k} vector and over all \mathbf{k} of magnitude k .

The advantage of the latter approach is a less aggressive scaling in the computation time, $\ell_{\text{max}}^5 V$ (number of $a_{\ell m}$ coefficients $\propto \ell_{\text{max}}^2$ times number of wave modes $\propto \ell_{\text{max}}^3 V$) in comparison with the former⁵ that goes as $\ell_{\text{max}}^7 V$. On the other hand, the disadvantage of the latter approach is that for each simulation we have to repeat the computations⁶. Nevertheless, we decided to adopt this method since the difference in scaling is particularly significant for the high resolution maps of interest in our studies. We also do not need more than one map for a given topology to evaluate the possibility of detection.

The topology does not affect local physics, so the equations governing the evolution of cosmological perturbations are left unchanged. Thus, to compute the response functions, $\Delta_\ell^T(k, \Delta\tau)$, one can use the publicly available CAMB code (Lewis, Challinor, & Lasenby 2000). A change of topology translates into a change of the modes that can exist in the universe. Therefore, we need to compute the response function only for a set of allowed wave numbers k . To speed up computations, we use in our code precomputed response functions. Then, the most time consuming part is the computation of the sum $\sum_{|\mathbf{k}|=k} Y_{\ell m}^*(\Omega_{\mathbf{k}}) \hat{e}_{\mathbf{k}}$.

The simulations do not include gravitational lensing of the CMB as the lensing deflection angle is small (Seljak 1996), $\sim 3'$, compared to the minimal angular scale taken into account in the simulations, $\sim 20'$. The effect of the finite thickness of the last scattering surface is included in the simulations through the response function, $\Delta_\ell^T(k, \Delta\tau)$, computed by CAMB. However, the effect starts to be important at angular scales smaller than $\sim 4'$ and will therefore not be studied here.

3.1 Requirements and numerical implementation

To study the signatures of a given topology, a CMB map is required with resolution comparable to the angular size of the beam profile used to smooth the *WMAP* W-band data (i.e. $\sim 20'$) to be analysed here (see Section 2). We have adopted $\ell_{\text{max}} = 500$ in our simulations. The dimension of the fundamental domain of the 3-torus was $L = 2c/H_0$, which is about three times less than diameter of the observable Universe i.e. $\sim 6.6c/H_0$. In such a universe there are many pairs of matched circles of different radii. The time needed for the generation of one such CMB map on a single processor with clock speed 3 GHz is about 42 hours.

⁵ the parity and symmetry relations can reduce by an order of magnitude the number of different elements in the matrix and computation time.

⁶ in the former case one need only generate a vector of Gaussian random numbers and multiply by the Choleski decomposed matrix. It is much faster than the full computation.

² available at <http://lambda.gsfc.nasa.gov>

³ <http://healpix.jpl.nasa.gov>

⁴ assuming zero mean of the CMB maps

4 SEARCHING FOR THE CIRCLES IN THE SKY

If light had sufficient time to cross the fundamental cell, an observer would see multiple copies of a single astronomical object. To have the best chance of seeing ‘around the universe’ we should look for multiple images of the furthest reaches of the universe. Searching for multiple images of the last scattering surface – the edge of the visible universe – is then a powerful way to constrain topology. Because the surface of last scattering is a sphere centred on the observer, each copy of the observer will come with a copy of the last scattering surface, and if the copies are separated by a distance less than the diameter of the last scattering surface, then they will intersect along circles. These are visible by both copies of the observer, but from opposite sides. The two copies are really one observer so if space is sufficiently small, the CMB radiation from the last scattering surface will demonstrate a pattern of hot and cold spots that match around the circles.

The idea of using these circles to study topology is due to Cornish, Spergel, & Starkman (1998). Therein, a statistical tool was developed to detect correlated circles in all sky maps of the CMB anisotropy – the circle comparison statistic

$$S_{p,r}^{\pm}(\alpha, \phi_*) = \frac{\langle 2T_p(\pm\phi)T_r(\phi + \phi_*) \rangle}{\langle T_p(\phi)^2 + T_r(\phi)^2 \rangle}, \quad (2)$$

where $\langle \rangle = \int_0^{2\pi} d\phi$ and $T_p(\pm\phi)$, $T_r(\phi + \phi_*)$ are the temperature fluctuations around two circles of angular radius α centered at different points, p and r , on the sky with relative phase ϕ_* . The sign \pm depends on whether the points along both circles are ordered in a clockwise direction (phased, sign $+$) or alternately whether along one of the circles the points are ordered in an anti-clockwise direction (anti-phased, sign $-$). This allows the detection of both orientable and non-orientable topologies. For orientable topologies the matched circles have anti-phased correlations while for non-orientable topologies they have a mixture of anti-phased and phased correlations. The statistic has a range over the interval $[-1, 1]$. Circles that are perfectly matched have $S = 1$, while uncorrelated circles will have a mean value of $S = 0$. To find matched circles for each radius α , the maximum value $S_{\max}^{\pm}(\alpha) = \max_{p,r,\phi_*} S_{p,r}^{\pm}(\alpha, \phi_*)$ is determined.

In order to speed up the computations, one can use the fast Fourier transform (FFT) along the circles, $T_p(\phi) = \sum_m T_{p,m} \exp(im\phi)$, and, by rewriting the statistic as $S_{p,r}^{\pm}(\alpha, \phi_*) = \sum_m s_m \exp(-im\phi_*)$, where $s_m = 2 \sum_m T_{p,m} T_{r,m}^* / \sum_n (|T_{p,n}|^2 + |T_{r,n}|^2)$, use inverse fast Fourier transform. It reduces the computational cost $S_{p,r}^{\pm}(\alpha, \phi_*)$ from $\sim N$ to $\sim N^{1/2} \log N$ operations, where N is number of pixels in the map.

In our studies we will use the statistic as modified in Cornish et al. (2004) to include weighting of the m th harmonic of the temperature around the p th circle $T_{p,m}$ by the factor $|m|$ that takes into account the number of degrees of freedom per mode:

$$S_{p,r}^+(\alpha, \phi_*) = \frac{2 \sum_m |m| T_{p,m} T_{r,m}^* e^{-im\phi_*}}{\sum_n |n| (|T_{p,n}|^2 + |T_{r,n}|^2)}, \quad (3)$$

where the Fourier coefficients $T_{p,m}$ are complex conjugated in the case of the $S_{p,r}^-$ statistic. Such weighting enhances the

contribution of small scale structure relative to the large scales fluctuations. It is especially important because the large scale fluctuations which are dominated by the integrated Sachs-Wolfe (ISW) effect. This can obscure the image of the last scattering surface and reduce the ability to recognise possible matched patterns on it.

The general search explores a six dimensional space: the location of the first circle centre, (θ_p, ϕ_p) , the location of the second circle centre, (θ_r, ϕ_r) , the angular radius of the circle α , and the relative phase of the two circles ϕ_* . The number of operations needed to search for circle pairs scales as $\sim N^3 \log N$; thus implementation of a matched circles test is computationally very intensive. Because of this we will restrict our analysis to a search for pairs of circles centered around antipodal points, so called back-to-back circles. Then, the search space can be reduced to four dimensions and the number of operations to $\sim N^2 \log N$. We will not search for nearly back-to-back circles as in Cornish et al. (2004), neither can we apply their hierarchical approach to speed up computations. In our case, we perform an analysis of high resolution maps ($\sim 20'$), so that the approach of initially degrading them to a lower resolution and then refining the search in higher resolution maps only for those circle pairs with the highest correlations risks missing some pairs of circles. As a consequence, our analysis is more computationally demanding than the analysis done by Cornish et al. (2004) preventing the study of a more general class of topologies. Although the back-to-back search can detect a large class of the topologies that we might hope to find, there remain those topologies that predict matched circles without antipodal configurations such as the Hantzsche-Wendt space for flat universes or the Picard space for hyperbolic universes (Aurich et al. 2004).

We used the HEALPIX scheme with resolution parameter $N_{\text{side}} = 512$ to define our search grid on the sky. To accommodate the use of the FFT approach, $n = 2^{r+1}$ points are used for each circle, where r corresponds to resolution parameter of the map given by $N_{\text{side}} = 2^r$. By definition this is also the angular resolution used to step through ϕ_* . For α , we used steps a little bit smaller than characteristic scale θ_c of coherent structures in the map, i.e. $2\theta_c/3$. The scale of coherence was approximated by the Full Width at Half Maximum (FWHM) of a gaussian beam profile used to smooth maps. The values of the temperature anisotropy at each point along the circle were interpolated based on values for the four nearest pixels with weights inversely proportional to the distances between a given point and the pixel centers. Other methods of interpolation can be used but we have verified that even using the temperature value of the nearest pixel does not change the value of the statistic significantly.

To draw any conclusions from an analysis based on the statistic $S_{\max}^{\pm}(\alpha)$ it is very important to correctly estimate the threshold for a statistically significant match of the circle pairs. The chance of random matches is inversely proportional to the number of coherent structures along the circles, therefore a false positive signal level of the statistic is especially large for circles with smaller radii. We used simulations of the maps with the same noise properties and smoothing scales as the WMAP data to establish the threshold such that fewer than 1 in 100 simulations would yield a false event.

It is important to note that the false detection level is smaller for higher resolution maps. Conversely, as shown by Cornish, Spergel, & Starkman (1998), the value of the statistic for matched circles

$$S_{\max} \approx \frac{\xi^2}{1 + \xi^2}, \quad (4)$$

depends on the ratio of the signal rms σ_s to the noise rms σ_n ratio, denoted ξ for the map, thus the efficiency of the statistic to detect matched circles is increased by smoothing the data. A smoothing scale should therefore be adopted that is a reasonable trade-off between these two requirements.

To eliminate the regions most contaminated by Galactic foreground residuals, we utilise the masks defined by the *WMAP* team. However, the statistic is very sensitive to the masking, particularly if a significant fraction of one or both circle pairs lies in the masked region. In this case, there is a significant probability to find a chance correlation of the temperature pattern between unmasked parts of the circles, thus increasing the false detection level. The effect is the most pronounced for circles with the largest radii, close to 90 degrees, as well with very small radii. To avoid this, we restrict our analysis to those pairs for which less than half the length of each circle is masked. Though, the statistic computed in this way is not optimal, it is much more robust with respect to masking. It should be noted that the dependence of the statistic on the cut could be avoided if the statistic were expressed as a function of the number of coherent structures along the circles. However, because our principal goal is to constrain the size of the Universe it is better to use the statistic determined as a function of circle radius.

Finally, Key et al. (2007) have suggested that the performance of the statistic (3) may be further improved by bandpass filtering the input map to minimise the anisotropy contribution from the ISW and Doppler terms which blur any signatures of topology present on the last scattering surface. We chose not to apply this kind of filtering because of possible complications arising from the interaction of the mask and the filter. Our analysis is enhanced by the use of high resolution maps rather than filtering.

5 RESULTS

Before beginning the search for pairs of matched circles in the *WMAP* data, we validated our algorithm using simulations of the CMB sky for a universe with 3-torus topology for which the dimension of the cubic fundamental domain $L = 2c/H_0$, and with cosmological parameters corresponding to the Λ CDM model (see Larson et al. 2010, Table 3) determined from the 7-year *WMAP* results. In particular, we verified that our code is able to find all pairs of matched circles in such map. The statistic $S_{\max}^-(\alpha)$ for the map is shown in Fig. 1. Note that the peak amplitudes in the statistic, corresponding to the temperature correlation for matched circles, decrease with radius of the circles. Cornish et al. (2004), noted that this is primarily caused by the Doppler term which becomes increasingly anticorrelated for circles with radius smaller than 45° . The temperature match on the last scattering surface will be also diluted by the ISW effect which comes from the evolution of the structures close

to the observer. However, to a large extent the m weighting used in the statistic (3) mitigates against this and prevents the statistic from being dominated by the large scales.

The intersection of the peaks in the matching statistic with the false detection level estimated for the W-band data (the same as in Fig. 3) defines the minimum radius of the correlated circles which can be detected for this map. The height of the peak with the smallest radius seen in Fig. 1 indicates that the minimum radius is about $\alpha_{\min} \approx 10^\circ$. To emphasise the advantage of using higher resolution data in the analysis, we also show the false detection level estimated for the ILC map (the same as in Fig. 2). In this case, the minimum radius for detectable matched circles is about $\alpha_{\min} \approx 25^\circ$.

The statistics for the *WMAP* ILC map are shown in Fig. 2. The map was analyzed on both the full sky and after applying the KQ85y7 mask (Gold et al. 2010). In the case of the full sky analysis, the S_{\max}^- statistic shows some excess for pairs of circle with large radii. Nevertheless, after removing the most foreground contaminated regions the statistic does not reveal any unusually large values. This indicates that residuals of the Galactic emission, especially in the Galactic plane, cannot be neglected in the analysis of matched circles.

It is interesting that similar behaviour is not seen for a full sky analysis of the first year *WMAP* ILC map. This probably explains why the importance of masking the most contaminated regions was not recognised in previous papers using the matched circles statistic, the only exception being the paper by Then (2006). However, because they studied only the first year *WMAP* data, they also came to the conclusion that the ILC map is good enough for the full sky analysis. We checked that the excess is not related to the bias correction (for residual foreground emission) applied to the 7-year ILC map by the *WMAP* team since this was not implemented for the first year data. Indeed, the excess remains present for the 7-year ILC constructed by simply coadding the individual frequency channels with the weights provided in Gold et al. (2010). Deeper studies of this problem are beyond the scope of this paper. Nevertheless, it provides a further warning against the naive use of a full sky ILC map for cosmological analysis, and particularly with respect to the two-point correlation function which is closely related to the statistic used here⁷.

The false detection level shown in Fig. 2 was estimated on the basis of 100 simulations of the ILC map with the KQ85y7 mask applied, assuming a simple-connected universe and established from the requirement that fewer than 1 in 100 simulations should yield a false match. We did not correct the simulated maps for the bias coming from the random correlation between the CMB and the Galactic foreground⁸, since the effect is small outside of the Galactic plane region. Moreover, such a correction does not appear to be reliably evaluated as demonstrated with simulations that have been generated using the same foreground templates as for the simulated ILC maps. Maps corrected in this way do

⁷ The remarks of Efstathiou, Ma, & Hanson (2010) regarding the lack of evidence for Galactic foreground residuals at low Galactic latitudes are only relevant for the ILC map when smoothed to 10° resolution.

⁸ so called ‘Cosmic Covariance’

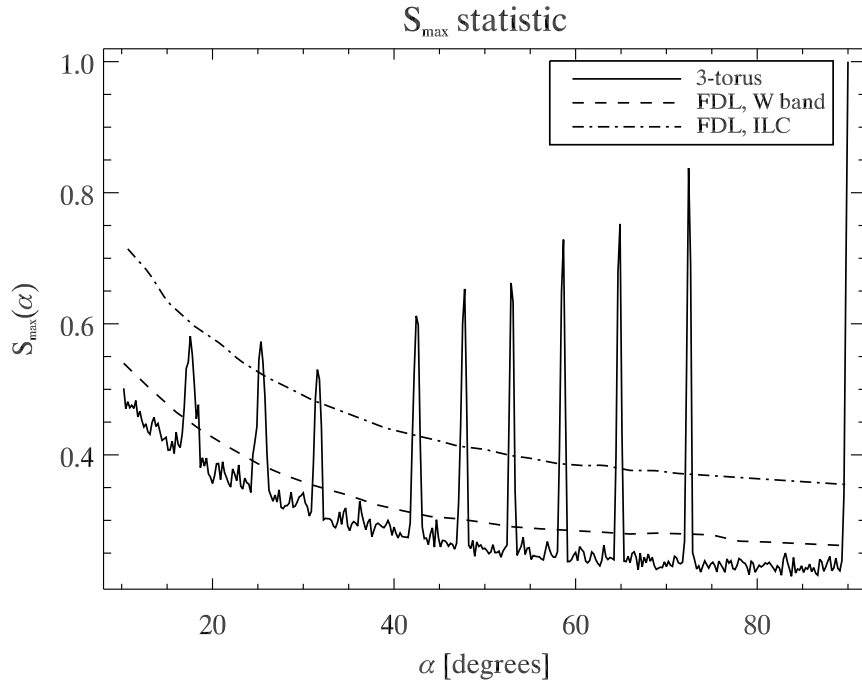


Figure 1. An example of the S_{\max}^- statistic for a simulated CMB map of universe with the topology of a cubic 3-torus with dimensions $L = 2 c/H_0$. The dashed and dot-dashed lines show the false detection level for the statistic estimated from 100 MC simulations of the WMAP 7-year W-band map (the same as in Fig. 3) and ILC map (the same as in Fig. 2), respectively.

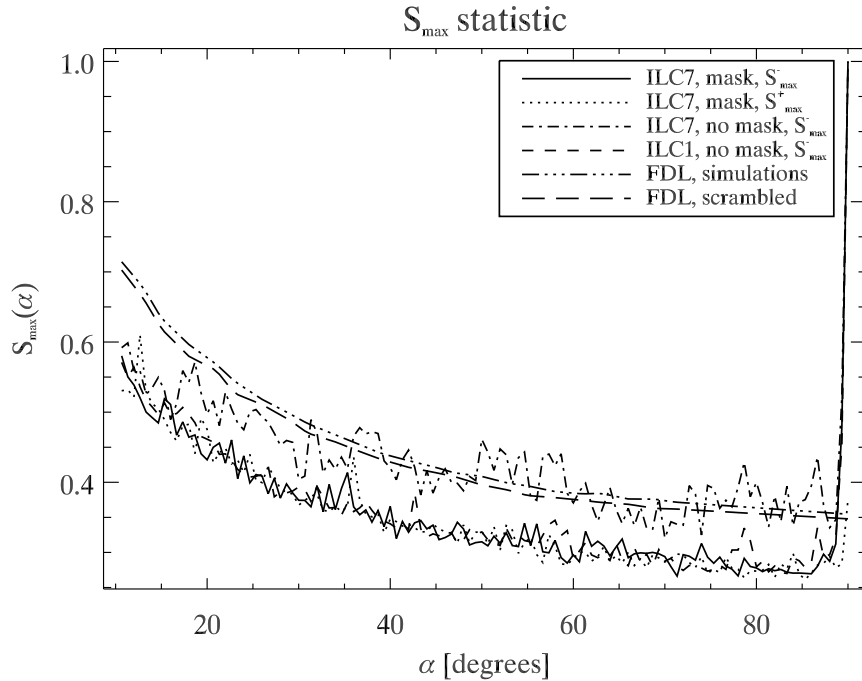


Figure 2. S_{\max}^{\pm} statistic for the WMAP 7-year ILC map. The solid and dotted lines show the statistics S_{\max}^- and S_{\max}^+ , respectively, for the ILC map masked with the KQ85y7 mask. The dash-dotted and dashed lines show the statistic S_{\max}^- for the 7-year and the first year ILC unmasked maps, respectively. The false detection level estimated from 100 MC simulations of the ILC map and by scrambling the $a_{\ell m}$ coefficients of the map are marked by dash-three dots and long dashed lines, respectively. The peak at 90° corresponds to a match between two copies of the same circle of radius 90° centered around two antipodal points.

not properly reflect uncertainties concerning details of the Galactic emission, especially in the Galactic plane.

For comparison we show also the false detection level estimated on the basis of a ‘scrambled’ version of the ILC map (i.e. by randomly exchanging the m spherical harmonic coefficients, $a_{\ell m}$, of the map at every ℓ) as in Cornish et al. (2004). However, we still applied the KQ85y7 mask for each ‘scrambled’ map to be consistent with simulations of the ILC data. As can be seen, the false detection level is slightly lower in this case. It is not surprising because the scrambling generates maps with the same two-point function and only different phase correlations that results in a smaller variance of the S -statistic than for an ensemble of simulated ILC maps.

In order to decrease the false detection level and be able to detect matched circles with smaller radius, we analyzed also the *WMAP* data with the highest angular resolution i.e. the W-band map, corrected for Galactic foregrounds and smoothed with a gaussian beam profile of $\text{FWHM} = 20'$ to decrease the noise level. The statistic for this map analysed with the KQ85y7 mask is shown in Fig. 3. As for the ILC map, the false detection level was estimated from 100 simulations of the W-band data.

We did not find any statistically significant correlation of circle pairs in either map. As seen in Fig. 1, the minimum radius at which the peaks expected for the matching statistic are larger than the false detection level is about $\alpha_{\min} \approx 10^\circ$ for the W-band map. Thus, we can exclude any topology that predicts matching pairs of back-to-back circles larger than this radius. This implies that in a flat universe described otherwise by the best-fit 7-year *WMAP* cosmological parameters, a lower bound on the size of the fundamental domain is $d = 2 R_{\text{LSS}} \cos(\alpha_{\min}) \simeq 27.9$ Gpc, where R_{LSS} is the distance to the last scattering surface.

Of course, the above constraints do not apply to those universes for which the orientation of the matched circles is impossible to detect due to partial masking on the sky. Examples of topologies which can be overlooked are so called slab and chimney spaces (Riazuelo et al. 2004a). For such topologies and appropriate configuration, all pairs of matched circles could lie in the Galactic plane that is removed by the mask. The probability of overlooking the circles depends on the specific topology and radii of the circles, so it is difficult to give a general expression. Nevertheless, one can suppose that it decreases as the fraction of the masked sky decreases.

6 CONCLUSIONS

We have studied constraints on the topology of the Universe using the method of matched circles as applied to the 7-year *WMAP* ILC map and the foreground-reduced W-band map. We paid special attention to three aspects of the analysis that have been neglected in previous studies – the application of a mask, the use of high resolution data and the estimation of the false detection level on the basis of detailed MC simulations of the sky maps.

The necessity for the application of a mask is due to the presence of residual Galactic foreground emission present even in the ILC map. These introduce a non-negligible effect on the matched circles statistic that is used for constraining

topology. However, the possibility to apply the analysis to masked maps yields the opportunity to more tightly constrain topology by using higher resolution, foreground corrected *WMAP* W-band data. Constraints on the topology depend significantly on the threshold for a significant match of the circle pairs. In order to estimate this correctly, we used 100 MC simulations of the ILC and W-band maps assuming a simply-connected universe. The level of false detection calibrated in this manner is slightly higher than that derived in Cornish et al. (2004) using a method in which the analyzed maps are resampled by shuffling their spherical harmonic coefficients. Although the difference is not very big, it is worth noting that the constraints on the size of Universe are overestimated if one uses a lower level of false detection.

The analysis of the *WMAP* W-band map, after correction using templates of Galactic foreground emission, did not reveal any significant correlations for pairs of back-to-back circles with a radius greater than $\sim 10^\circ$. This substantially extends the previous constraint on the minimum radius of detectable matched circles given by Key et al. (2007) of 20° . It also places a lower bound on the size of fundamental domain of about 27.9 Gpc for a flat universe described by the best-fit 7-year *WMAP* cosmological parameters. Although this constraint concerns only those universes with such dimensions and orientation of the fundamental domain with respect to the mask that allow the detection of pairs of matched circles, the probability of overlooking circle pairs is rather low for the KQ85y7 mask that removes only a relatively small fraction of the sky.

Of course, observations of the CMB with higher angular resolution and significantly lower noise level by the *Planck* satellite may yield even tighter constraints on the topology of the Universe. However, one should bear in mind that the possible improvement in the lower bound on the size of the Universe will not be substantial. The current constraint is not much smaller than the diameter of the observable Universe $2 R_{\text{LSS}} = 28.3$ Gpc, which imposes an upper limit on the size of the fundamental domain that it is possible to detect using the method of matched circles. The only significant improvement might be related to improved modeling of the Galactic emission allowing the application of a smaller mask approaching closer to the Galactic plane. This would minimize the probability of overlooking topologies with matched circles that are hidden within the masked region of the sky.

Finally, as in Cornish et al. (2004), the studies could also be extended to search for nearly back-to-back circle pairs. However, the much higher computational requirements for the analysis of high resolution maps make such studies difficult and extremely time-consuming. Nevertheless, we can hope that the steadily increasing speed of processors and availability of larger computational resources will make such computations feasible in the coming years, thus allowing a final resolution of the problem of the topology of our Universe.

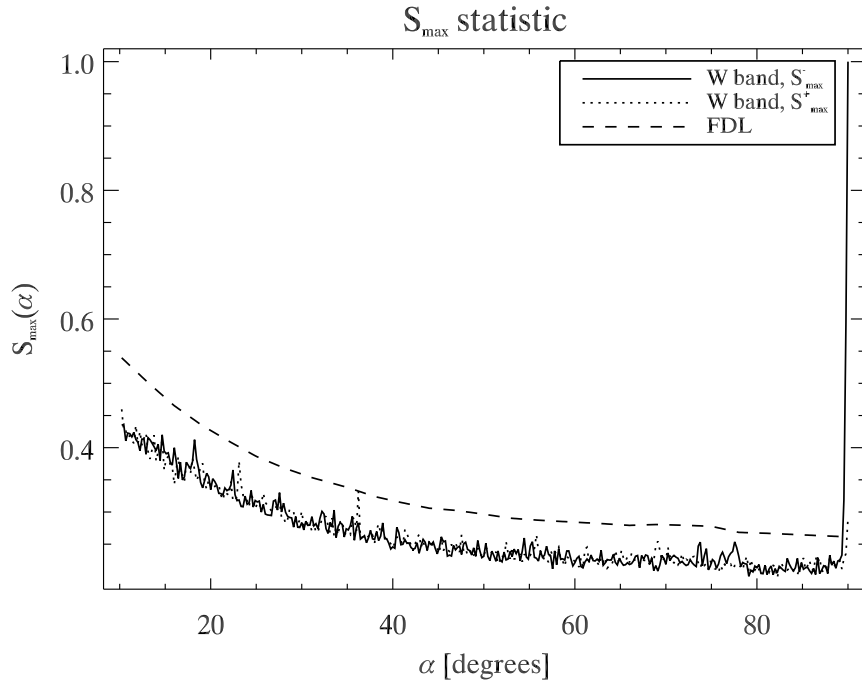


Figure 3. S_{\max}^{\pm} statistic for the *WMAP* 7-year W-band map. Solid and dotted lines show the statistics S_{\max}^{-} and S_{\max}^{+} , respectively, for the W-band map masked with the KQ85y7 mask. The dashed line is the false detection level estimated from 100 MC simulations. The peak at 90° corresponds to a match between two copies of the same circle of radius 90° centered around two antipodal points.

ACKNOWLEDGMENTS

We acknowledge use of *CAMB*⁹ (Lewis, Challinor, & Lasenby 2000) and the *HEALPIX* software (Górski et al. 2005) and analysis package for deriving the results in this paper. We acknowledge the use of the Legacy Archive for Microwave Background Data Analysis (LAMBDA). Support for LAMBDA is provided by the NASA Office of Space Science. The authors acknowledge the use of version 1.6.6 of the Planck Sky Model, developed by the Component Separation Working Group (WG2) of the *Planck* Collaboration (Leach et al. 2008; Betoule et al. 2009). Part of the computations were performed at Interdisciplinary Center for Mathematical and Computational Modeling at Warsaw University within a grant of computing time no. G27-13. This research was supported by the Agence Nationale de Recherche (ANR-08-CEXC-0002-01).

REFERENCES

- Aurich R., Lustig S., Steiner F., Then H., 2004, *CQGra*, 21, 4901
- Aurich R., Lustig S., Steiner F., 2005, *CQGra*, 22, 2061
- Aurich R., Lustig S., Steiner F., 2006, *MNRAS*, 369, 240
- Betoule M., Pierpaoli E., Delabrouille J., Le Jeune M., Cardoso J.-F., 2009, *A&A*, 503, 691
- Copi C. J., Huterer D., & Starkman G. D., 2004, *Phys. Rev. D.*, 70, 043515
- Cornish N. J., Spergel D. N., Starkman G. D., 1998, *CQ-Gra*, 15, 2657
- Cornish N. J., Spergel D. N., Starkman G. D., Komatsu E., 2004, *PhRvL*, 92, 201302
- de Oliveira-Costa A., Tegmark M., Zaldarriaga M., Hamilton A. 2004, *Phys. Rev. D.*, 69, 063516
- Efstathiou G., Ma Y.-Z., Hanson D., 2010, *MNRAS*, 407, 2530
- Eriksen H. K., Hansen F. K., Banday A. J., Górski K. M., & Lilje P. B., 2004, *ApJ*, 605, 14
- Gold B., et al., 2010, arXiv, arXiv:1001.4555
- Górski K. M., Hivon E., Banday A. J., Wandelt B. D., Hansen F. K., Reinecke M., & Bartelmann M., 2005, *ApJ*, 622, 759
- Hansen F. K., Banday A. J., & Górski K. M. 2004, *MNRAS*, 354, 641
- Jarosik N., et al., 2010, arXiv, arXiv:1001.4744
- Key J. S., Cornish N. J., Spergel D. N., Starkman G. D., 2007, *PhRvD*, 75, 084034
- Kunz M., Aghanim N., Cayon L., Forni O., Riazuelo A., Uzan J. P., 2006, *PhRvD*, 73, 023511
- Kunz M., Aghanim N., Riazuelo A., Forni O., 2008, *PhRvD*, 77, 023525
- Larson D., et al., 2010, arXiv, arXiv:1001.4635
- Leach S. M., et al., 2008, *A&A*, 491, 597
- Lewis A., Challinor A., Lasenby A., 2000, *ApJ*, 538, 473
- Phillips N. G., Kogut A., 2006, *ApJ*, 645, 820
- Riazuelo A., Uzan J.-P., Lehoucq R., Weeks J., 2004a, *PhRvD*, 69, 103514
- Riazuelo A., Weeks J., Uzan J.-P., Lehoucq R., Luminet J.-P., 2004b, *PhRvD*, 69, 103518
- Schwarz D. J., Starkman G. D., Huterer D., Copi, C. J.,

⁹ <http://camb.info/>

2004, Phys. Rev. Lett., 93, 221301

Seljak U., 1996, ApJ, 463, 1

Then H., 2006, MNRAS, 373, 139